



**Functional Specialization in Rhesus Monkey
Auditory Cortex**

Biao Tian, *et al.*
Science **292**, 290 (2001);
DOI: 10.1126/science.1058911

**The following resources related to this article are available online at
www.sciencemag.org (this information is current as of August 20, 2007):**

Updated information and services, including high-resolution figures, can be found in the online version of this article at:

<http://www.sciencemag.org/cgi/content/full/292/5515/290>

Supporting Online Material can be found at:

<http://www.sciencemag.org/cgi/content/full/292/5515/290/DC1>

This article **cites 21 articles**, 9 of which can be accessed for free:

<http://www.sciencemag.org/cgi/content/full/292/5515/290#otherarticles>

This article has been **cited by** 166 article(s) on the ISI Web of Science.

This article has been **cited by** 55 articles hosted by HighWire Press; see:

<http://www.sciencemag.org/cgi/content/full/292/5515/290#otherarticles>

This article appears in the following **subject collections**:

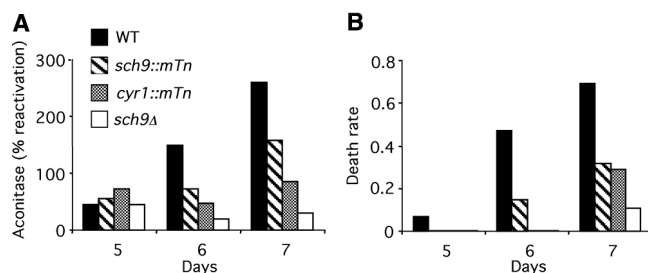
Neuroscience

<http://www.sciencemag.org/cgi/collection/neuroscience>

Information about obtaining **reprints** of this article or about obtaining **permission to reproduce this article** in whole or in part can be found at:

<http://www.sciencemag.org/about/permissions.dtl>

Fig. 4. Mutations in *cyr1* and *sch9* delay the reversible inactivation of the superoxide-sensitive enzyme aconitase in the mitochondria. **(A)** Mitochondrial aconitase percent reactivation after treatment of whole-cell extracts of yeast removed from cultures at day 5 through 7 with agents (iron and Na₂S) able to reactivate superoxide inactivated [4Fe-4S] clusters. **(B)** Death rate reported as the fraction of cells that lose viability in the 24-hour period following the indicated day.



norhabditis elegans age-1 and *daf-2* mutations extend the life-span in adult organisms by 65 to 100%, by decreasing AKT-1/AKT2 signaling and activating transcription factor DAF-16 (14, 18, 23). These changes are associated with the induction of superoxide dismutase (MnSOD), catalase, and the heat shock proteins HSP70 and HSP90 (14, 17). A role for oxidants in the aging of *C. elegans* was confirmed by the extended survival of wild-type worms treated with small synthetic SOD/catalase mimetics (24). Thus, the yeast Gpr1/Cyr1/PKA/Msn2/4-Sch9/Rim15 and the *C. elegans* DAF-2/AGE-1/AKT/DAF16 pathways play similar roles in regulating longevity and stress resistance (14). Analogously, a *Drosophila* line with a mutation in the heterotrimeric guanosine triphosphate-binding protein (G protein)-coupled receptor homolog *MTH* gene displays a 35% increase in life-span and is resistant to starvation and paraquat toxicity (25). Furthermore, in flies, aconitase undergoes age-dependent oxidation and inactivation (26), and the overexpression of *SOD1* increases survival by up to 40% (27, 28). A mutation in a signal-transduction gene also increases resistance to stress and lengthens survival in mammals. A knockout mutation in the signal transduction p66^{SHC} gene increases resistance to paraquat and hydrogen peroxide and extends survival by 30% in mice (29).

We propose that yeast Sch9 and PKA and worm AKT-1/AKT-2 evolved from common ancestors that regulated metabolism, stress resistance, and longevity in order to overcome periods of starvation. Analogous mechanisms triggered by low nutrients may be responsible for the extended longevity of dietary restricted rodents (3). The phenotypic similarities of long-lived mutants ranging from yeast to mice (1, 2), and the role of the conserved yeast Sch9 and PKA and mammalian Akt/PKB in glucose metabolism, raise the possibility that the fundamental mechanism of aging may be conserved from yeast to humans.

References and Notes

1. T. Finkel, N. J. Holbrook, *Nature* **408**, 239 (2000).
2. V. D. Longo, *Neurobiol. Aging* **20**, 479 (1999).
3. C. E. Finch, *Longevity, Senescence, and the Genome* (University Press, Chicago, 1990).
4. J. W. Vaupel *et al.*, *Science* **280**, 855 (1998).

5. N. K. Egilmez, S. M. Jazwinski, *J. Bacteriol.* **171**, 37 (1989).
6. D. Sinclair, K. Mills, L. Guarente, *Annu. Rev. Microbiol.* **52**, 533 (1998).
7. S.-J. Lin, P.-A. Defossez, L. Guarente, *Science* **289**, 2126 (2000).
8. V. D. Longo, L. M. Ellerby, D. E. Bredesen, J. S. Valentine, E. B. Gralla, *J. Cell Biol.* **137**, 1581 (1997).
9. L.-L. Liou, P. Fabrizio, V. N. Moy, J. W. Vaupel, J. S. Valentine, E. Butler Gralla, and V. D. Longo, unpublished results; L.-L. Liou, thesis, University of California Los Angeles, Los Angeles (1999).
10. M. Werner-Washburne, E. L. Braun, M. E. Crawford, V. M. Peck, *Mol. Microbiol.* **19**, 1159 (1996).
11. V. D. Longo, E. B. Gralla, J. S. Valentine, *J. Biol. Chem.* **271**, 12275 (1996).
12. V. D. Longo, L. L. Liou, J. S. Valentine, E. B. Gralla, *Arch. Biochem. Biophys.* **365**, 131 (1999).
13. Transposon mutagenesis and allele rescue were performed as described [P. Ross-Macdonald *et al.*, *Methods Enzymol.* **303**, 512 (1999)] using the yeast insertion library provided by M. Snyder.

14. Supplementary material is available at www.sciencemag.org/cgi/content/1059497/DC1
15. K. A. Morano, D. J. Thiele, *EMBO J.* **18**, 5953 (1999).
16. J. M. Thevelein, J. H. de Winde, *Mol. Microbiol.* **33**, 904 (1999).
17. L. Guarente, C. Kenyon, *Nature* **408**, 255 (2000).
18. S. Paradis, M. Ailion, A. Toker, J. H. Thomas, G. Ruvkun, *Genes Dev.* **13**, 1438 (1999).
19. E. S. Kandel, N. Hay, *Exp. Cell Res.* **253**, 210 (1999).
20. J. A. Flattery-O'Brien, C. M. Grant, I. W. Dawes, *Mol. Microbiol.* **23**, 303 (1997).
21. I. Pedruzzi, N. Burckert, P. Egger, C. De Virgilio, *EMBO J.* **19**, 2569 (2000).
22. P. R. Gardner, I. Fridovich, *J. Biol. Chem.* **267**, 8757 (1992).
23. T. E. Johnson, *Science* **249**, 908 (1990).
24. S. Melov *et al.*, *Science* **289**, 1567 (2000).
25. Y.-J. Lin, L. Seroude, S. Benzer, *Science* **282**, 943 (1998).
26. L. J. Yan, R. L. Levine, R. S. Sohal, *Proc. Natl. Acad. Sci. U.S.A.* **94**, 11168 (1997).
27. T. L. Parkes *et al.*, *Nature Genet.* **19**, 171 (1998).
28. J. Sun, J. Tower, *Mol. Cell Biol.* **19**, 216 (1999).
29. E. Migliaccio *et al.*, *Nature* **402**, 309 (1999).
30. Supported by NIH grants AG 08761-10 (J. W. Vaupel, V.D.L.) and AG09793 (T. H. McNeill), by an American Federation of Aging Research grant (V.D.L.), and by a John Douglas French Alzheimer's Foundation grant (V.D.L.). We thank J. Martin and G. Fenimore for their generous donations, C. Finch and E. Gralla for careful reading of the manuscript, D. Thiele, J. Hirsh, M. Carlson, S. Garrett, A. Mitchell, and J. Field for providing yeast plasmids, J. Vaupel for generously allowing the use of Max Planck Institute facilities and instruments, and M. Wei for performing data analysis.

1 February 2001; accepted 15 March 2001
 Published online 5 April 2001;
 101126/science.1059497
 Include this information when citing this paper.

Functional Specialization in Rhesus Monkey Auditory Cortex

Biao Tian, David Reser, Amy Durham, Alexander Kustov, Josef P. Rauschecker*

Neurons in the lateral belt areas of rhesus monkey auditory cortex prefer complex sounds to pure tones, but functional specializations of these multiple maps in the superior temporal region have not been determined. We tested the specificity of neurons in the lateral belt with species-specific communication calls presented at different azimuth positions. We found that neurons in the anterior belt are more selective for the type of call, whereas neurons in the caudal belt consistently show the greatest spatial selectivity. These results suggest that cortical processing of auditory spatial and pattern information is performed in specialized streams rather than one homogeneously distributed system.

Hearing plays a dual role in the identification of sounds and in their localization. Although it is undisputed that auditory cortex participates in the analysis of spectro-temporal patterns for the identification of complex sound objects, including speech and music, the neural basis of auditory spatial perception re-

mains a matter of controversy. Brainstem-structures play a significant role in the processing of binaural cues, which contain important information for sound localization (1). However, lesions of auditory cortex also impair auditory spatial analysis (2, 3). With the recent discovery of multiple cochleotopic maps in nonprimary auditory cortex of the rhesus monkey (4, 5), the question arises whether neurons in some of these areas show greater specificity for sound source location than in others. This could indicate the existence of a specialized cortical stream for the processing of auditory space, similar to what

Georgetown Institute for Cognitive and Computational Sciences, Department of Physiology and Biophysics, Georgetown University Medical Center, Washington, DC 20007, USA.

*To whom correspondence should be addressed. E-mail: rauschej@georgetown.edu

REPORTS

has been postulated for the visual cortical system (6). Alternatively, auditory spatial information may be encoded in a completely homogeneous, distributed manner with each cortical area contributing equally to auditory spatial perception.

One of the cortical systems in the macaque identified beyond the primary-like core areas of the auditory cortex is the lateral belt (7, 8). It contains at least three areas: an anterolateral (AL), a middle lateral (ML), and a caudolateral (CL) area (4). CL and AL receive largely independent and parallel input from different areas of the auditory core (A1 and R, respectively) and are only weakly interconnected (9, 10). CL in addition has strong connections with the caudomedial area (CM) and projects to a different target region of the prefrontal cortex than AL (10, 11). ML, situated between AL and CL and connected with both, shows attributes of an intermediate stage between core and belt (10, 12). Neurons in all three lateral belt areas respond better to complex sounds than to pure tones (4, 13). Stimulus preferences include band-passed noise (BPN), frequency-modulated sweeps, and species-specific vocalizations (“monkey calls,” or MCs). The caudal part of the superior temporal gyrus (STG) contains neurons that are spatially tuned to the location of a sound stimulus presented in free field (14, 15). We therefore compared the spatial selectivity of single neurons in the caudal belt region of four rhesus monkeys with that in more anterior areas. At the same time, by using MCs for stimulation, we determined the extent to which neurons in the various belt regions differ with regard to their specificity for different kinds of sound.

First, BPN bursts of variable bandwidth centered at different frequencies were used to map the lateral belt areas on the STG to determine the borders of AL, ML, and CL (4, 16). Then, a standard battery of seven selected MCs (17) was used to test the spatial tuning of the same neurons in azimuth and evaluate their specificity for MCs (Fig. 1). To determine a neuron’s selectivity for the seven spatial positions with the seven MCs, we assembled a “response profile” on the basis of 490 stimulus presentations (18). In comparing response profiles of cells in AL (Fig. 2A) with those in CL (Fig. 2B), it became evident that CL responses were often highly specific for spatial position, whereas AL neurons usually responded equally to sounds from all locations. Some of the spatially selective CL neurons were also highly specific for the type of MC presented (Fig. 2B, right), whereas others showed broader tuning in that domain. AL neurons, by contrast, seemed overall to be more specific for the kind of MC regardless of where in space it was presented. Because only a limited azimuth range (120°) was tested, the overall number of spatially

tuned neurons was almost certainly underestimated, but this was equally true for all three areas. Despite the different spectral bandwidth of the calls, there was no overall ten-

dency for any of the call types to be associated with spatial-tuning width, nor was there any dependency of spatial-tuning width on the best center frequency (BF) of the neurons

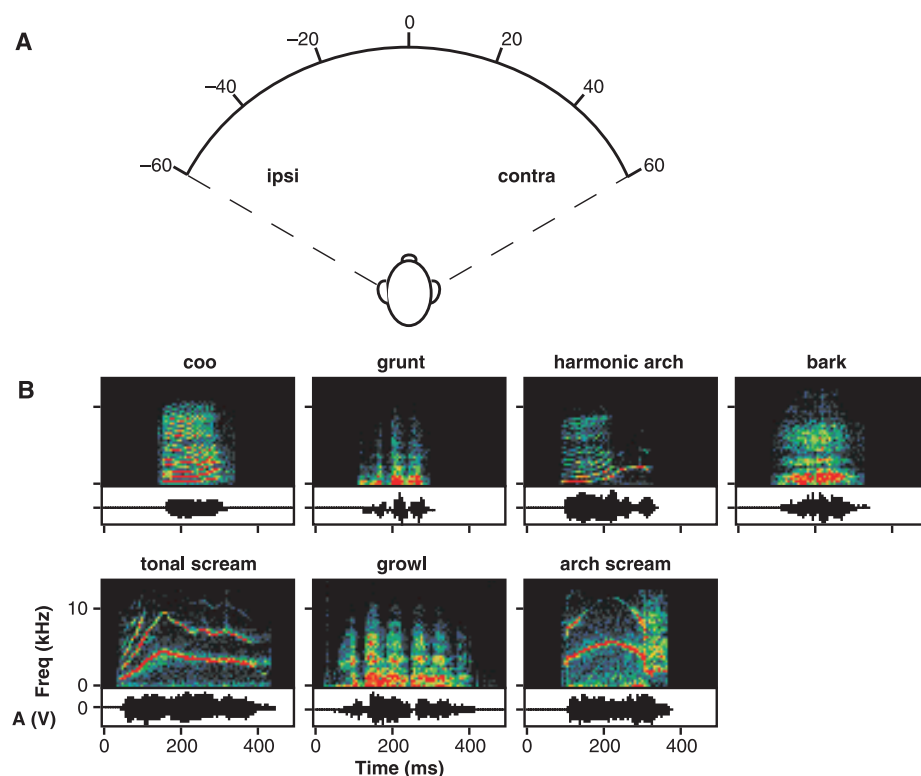


Fig. 1. Testing of spatial tuning in single neurons of macaque auditory belt cortex. (A) Loudspeakers set up in near-free field at the height of the monkey’s ears (zero elevation) in seven different azimuth positions. The calibrated speakers were mounted in 20° steps on a stationary horizontal hoop with a radius of 1.14 m, thus spanning a range of $\pm 60^\circ$ from the center of the animal’s head. (B) Spectrograms of the seven standard monkey calls that were used for stimulation.

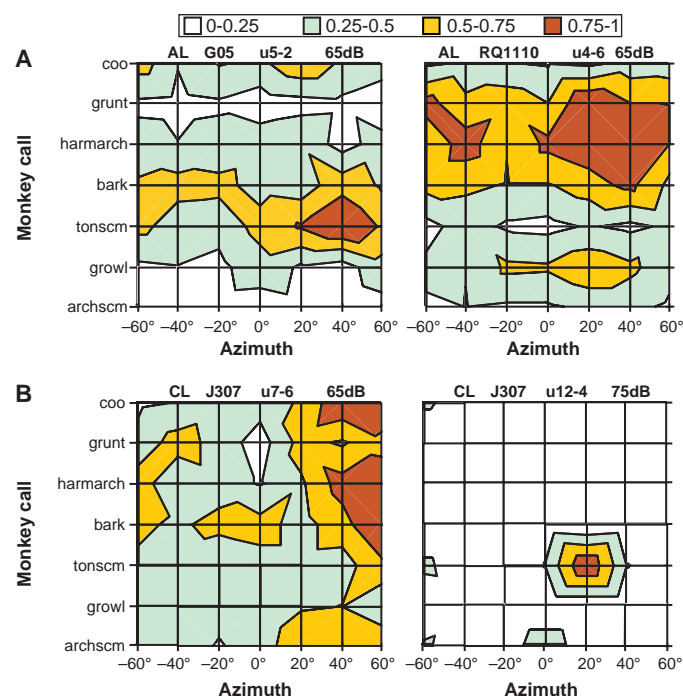


Fig. 2. Response profiles of single neurons in areas AL (A) and CL (B) of macaque monkey auditory cortex. Two representative examples from each area are shown. The selectivity of these neurons for the seven communication calls is displayed along the vertical axes, and selectivity across the seven spatial positions along the horizontal axes. The 49 individual responses were plotted according to the color scale shown at the top. For display purposes, linear interpolation was performed between data points.

Fig. 3. Maps of spatial selectivity in the lateral auditory belt from two monkeys. Spatial half-width is displayed on a color scale from yellow (most selective) to blue (least selective), as indicated at the bottom of the right panel. Borders between cortical areas AL, ML, and CL (dashed lines) were determined by mapping best center frequencies with band-passed noise bursts along the lateral sulcus (ls). Electrode penetrations are denoted by the letter "p" followed by a number and are projected onto a digital picture of the cortical surface in each animal showing vascularization pattern and major sulci (sts: superior temporal sulcus).

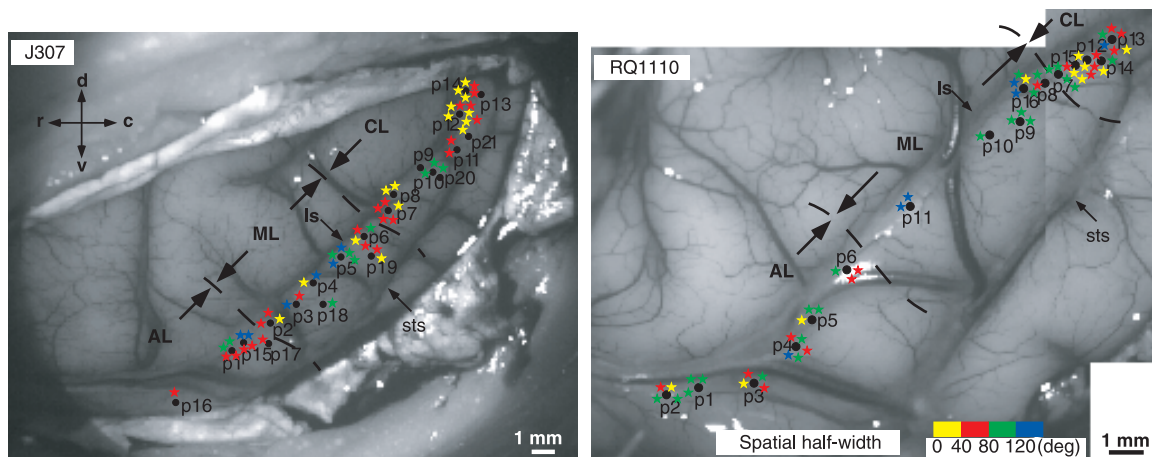
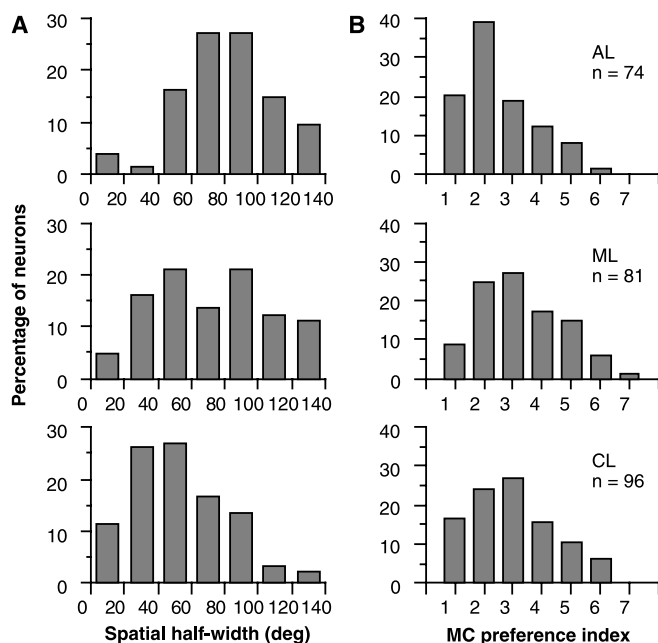


Fig. 4. Distribution of spatial half-width (A) and monkey call preference index (B) in areas AL, ML, and CL. Summary data from all four monkeys are shown in histogram form. The number of units recorded in each area is given on the right. Neurons in CL show significantly greater spatial selectivity than neurons in AL or ML. By contrast, neurons in AL are more selective for monkey calls than neurons in either of the other areas.



($r^2 = 0.002$, $P = 0.4456$). Selectivity for MCs was also not simply a function of BF_c , because neurons selective for different types of calls were found in all sections of the cochleotopic maps within the lateral belt [MC preference index (MCPI) versus BF_c : $r^2 = 0.013$; $P = 0.0761$]. Thus, MC selectivity is generated by complex integrations in both frequency and time (4, 13).

Mapping of spatial selectivity along the cortical surface in individual monkeys again demonstrates that neurons with great spatial selectivity are concentrated in the caudal belt (Fig. 3). Great care was taken to collect an equal amount of data from either end of the belt region (19). The interindividual variability of both spatial and MC selectivity was small in each area ($P > 0.05$, Kruskal-Wallis, $df = 3$), so individual data sets could be combined for further analysis.

The main results of the study are summarized in Fig. 4. Comparison of spatial tuning (Fig. 4A) shows that CL neurons were by far the most sharply tuned and AL neurons were most broadly tuned. ML, commensurate with its anatomical status, fell in the middle of the tuning range with a hint of a bimodal distribution. The difference between the three areas in spatial half-width was highly significant when compared with a nonparametric analysis of variance ($P < 0.0001$, Kruskal-Wallis, $df = 2$). The same result was obtained when CL was compared individually with AL and ML ($P < 0.0001$ and $P = 0.002$, respectively; Mann-Whitney U test) (20). Comparison of MC selectivity (Fig. 4B) showed AL to be more selective than both ML and CL ($P = 0.0006$ and $P = 0.0287$, respectively; Mann-Whitney U test). This difference was also highly significant when all three areas

were compared together ($P = 0.0026$, Kruskal-Wallis, $df = 2$). MC selectivity in CL, when present, was often associated with the prevailing high selectivity in the spatial domain.

Thus, we find a clear dissociation of auditory spatial tuning between anterior and caudal belt in rhesus monkey auditory cortex. Spatial selectivity is greatest in CL and lowest in AL. Our findings represent physiological evidence for a functional specialization within the auditory cortex of primates and support the idea of processing streams at higher levels of the auditory system (11, 21). Auditory spatial information is known to be processed in posterior parietal (22, 23) as well as dorsolateral prefrontal cortex (PFC) (11, 22). The caudal belt provides direct input to both of these regions (11, 13, 24) and could thus be regarded as the origin of a dorsally directed "where" stream for auditory processing. The finding of an increased concentration of spatially tuned neurons in the caudal belt is consistent with other studies (14, 15, 25), which demonstrate that this organizational feature is indeed associated with sound localization behavior. Other aspects of auditory spatial perception, in which the dorsal cortical pathway may be involved, include distance perception (26) and analysis of auditory motion (23).

By contrast, AL seems to be part of an auditory-processing stream that is rostrally directed and continues into ventral and orbital PFC (11, 13, 27). The latter route is supported by recent human imaging data that demonstrate an antero-ventral "what" stream for the analysis of human speech (28–30). However, our results suggest that signals used for auditory communication are also related to the caudal STG, where they are combined, at the single-unit level, with information about the location of sounds in space. This type of neuron could play an important role in sound

segregation (and possibly identification of speakers) on the basis of spatial cues (31, 32).

The usefulness of natural complex sounds as stimuli in higher auditory areas has been emphasized previously (4, 13). The selectivity for specific types of MCs, as found in auditory belt neurons, is higher than expected. However, even in AL, neurons rarely responded to a single call [although they sometimes responded to calls within the same phonetic category (33)]. This suggests that AL is still far from the end-stage in processing auditory objects, and recordings from awake animals in even more anterior and lateral areas of the STG may be promising. On the other hand, lack of extreme selectivity may also indicate that complex auditory patterns, such as vocalizations, are coded by networks of neurons rather than a single cell.

References and Notes

1. M. Konishi, T. T. Takahashi, H. Wagner, W. E. Sullivan, C. E. Carr, in *Auditory Function. Neurobiological Bases of Hearing*, G. M. Edelman, W. E. Gall, W. M. Cowan, Eds. (Wiley, New York, 1988), pp. 721–745.
2. W. M. Jenkins, M. M. Merzenich, *J. Neurophysiol.* **52**, 819 (1984).
3. H. E. Heffner, R. S. Heffner, *J. Neurophysiol.* **64**, 915 (1990).
4. J. P. Rauschecker, B. Tian, M. Hauser, *Science* **268**, 111 (1995).
5. J. H. Kaas, T. A. Hackett, M. J. Tramo, *Curr. Opin. Neurobiol.* **9**, 164 (1999).
6. L. G. Ungerleider, M. Mishkin, in *Analysis of Visual Behaviour*, D. J. Ingle, M. A. Goodale, R. J. W. Mansfield, Eds. (MIT Press, Cambridge, MA, 1982), pp. 549–586.
7. D. N. Pandya, E. H. Yeterian, in *Cerebral Cortex*, A. Peters, E. G. Jones, Eds. (Plenum, New York, 1985), vol. 4, pp. 3–61.
8. A. Morel, P. E. Garraghty, J. H. Kaas, *J. Comp. Neurol.* **335**, 437 (1993).
9. E. G. Jones, E. Dell’Anna, M. Molinari, E. Rausell, T. Hashikawa, *J. Comp. Neurol.* **362**, 153 (1995).
10. T. A. Hackett, I. Stepniewska, J. H. Kaas, *J. Comp. Neurol.* **394**, 475 (1998).
11. L. M. Romanski et al., *Nature Neurosci.* **2**, 1131 (1999).
12. T. A. Hackett, I. Stepniewska, J. H. Kaas, *J. Comp. Neurol.* **400**, 271 (1998).
13. J. P. Rauschecker, *Curr. Opin. Neurobiol.* **8**, 516 (1998).
14. J. P. Rauschecker, B. Tian, T. Pons, M. Mishkin, *J. Comp. Neurol.* **382**, 89 (1997).
15. G. H. Recanzone, D. C. Guard, M. L. Phan, T. K. Su, *J. Neurophysiol.* **83**, 2723 (2000).
16. A total of 80 penetrations perpendicular to the open surface of the STG were made with lacquer-coated tungsten electrodes along the lateral sulcus of four rhesus monkeys (*Macaca mulatta*), lightly anesthetized with isoflurane (0.5 to 1.5%) and nitrous oxide (50%). All studies were performed within a double-walled sound-proof chamber (3.05 m by 2.85 m by 1.98 m) whose inside walls were covered with 4-inch-thick acoustic foam to minimize standing waves and echoes. Single units were isolated with the aid of a window discriminator and a slicer unit (34). BF_c of each unit was determined with BPN stimuli presented through the center speaker. The borders between two adjacent belt areas were identified from the reversal point of the BF_c . BPN stimuli were 200 ms long with a rise-and-fall time of 5 ms. All sounds were energy-matched on the basis of root-mean-square values and were played at sound pressure levels of 45 to 75 dB, i.e., well in the suprathreshold range. When several levels were tested, the best response was used for analysis.
17. Digitized calls recorded from free-ranging monkeys

were used for stimulation. The calls can be subdivided phonetically into three major groups: tonal, harmonic, and noisy calls (35).

18. Each of the seven MCs was played back in succession at all seven positions, from the most contra- to the most ipsilateral, and this was repeated 10 times for each call. MC types were presented in a fixed order, harmonic or tonal calls alternating with noisy calls (see Fig. 1B and the vertical scale of Fig. 2). An alternative design, in which positions and MCs were completely randomized, was abandoned in favor of the standardized sequence, because it poses the risk of total data loss when a neuron is lost prematurely. A comparison of the results from random and standardized stimulus presentation in several neurons did not reveal any significant differences, and stability of recordings was always monitored from raster displays. Only complete data sets from a total of 251 units were used. The spikes in response to stimulation were added up into 49 MC- and position-specific peristimulus time histograms (PSTHs). All PSTHs had a prestimulus interval of 500 ms, from which baseline activity was determined. Net responses were quantified from averaged peak firing rates with a 40-ms “sliding window” and normalized. The MC that elicited the maximal response was defined as the preferred monkey call, and the spatial position of that call as the preferred azimuth. An MCPI was defined as the number of MCs to which a neuron yielded a response >50% of the maximum at the preferred azimuth. Spatial selectivity was determined by the width of the half-maximal response to the preferred monkey call across azimuth. Neurons were considered spatially tuned if their response fell to less than 50% of the maximum at any other spatial position and were classified as “contra-field,” “ipsi-field,” or “single-peak” (36). Of all preferred azimuths, 59% fell into the contralateral, 32% into the ipsilateral hemifield, and 9% were straight ahead (0°). This distribution was similar in all three belt areas ($P > 0.1$, χ^2 -test).
19. One of the monkeys was prepared for semichronic recording (37), so that both CL and AL could be mapped exhaustively in repeated sessions. A recording chamber and head bolt were mounted on the animal’s skull in a single aseptic surgery under gas anesthesia. Fifteen recording sessions, each lasting 6

to 8 hours, were subsequently performed under the same conditions as in the acute experiments.

20. When measured with BPN bursts, spatial half-width was very similar ($n = 38$; $P > 0.05$, Wilcoxon signed rank test for pairwise comparisons) (33), and the difference between AL and CL, despite the small sample size, was still significant ($P < 0.05$, Mann-Whitney U test).
21. J. P. Rauschecker, B. Tian, *Proc. Natl. Acad. Sci. U.S.A.* **97**, 11800 (2000).
22. K. O. Bushara et al., *Nature Neurosci.* **2**, 759 (1999).
23. T. D. Griffiths et al., *Nature Neurosci.* **1**, 74 (1998).
24. J. W. Lewis, D. C. Van Essen, *J. Comp. Neurol.* **428**, 112 (2000).
25. L. Leinonen, J. Hyvärinen, A. R. A. Sovijärvi, *Exp. Brain Res.* **39**, 203 (1980).
26. M. S. A. Graziano, L. A. J. Reiss, C. G. Gross, *Nature* **397**, 428 (1999).
27. T. A. Hackett, I. Stepniewska, J. H. Kaas, *Brain Res.* **817**, 45 (1999).
28. J. R. Binder et al., *Cereb. Cortex* **10**, 512 (2000).
29. P. Belin, R. J. Zatorre, P. Lafaille, P. Ahad, B. Pike, *Nature* **403**, 309 (2000).
30. S. K. Scott, C. C. Blank, S. Rosen, R. J. S. Wise, *Brain* **123**, 2400 (2000).
31. D. E. Broadbent, *Perception and Communication* (Pergamon, London, 1958).
32. A. S. Bregman, *Auditory Scene Analysis* (MIT Press, Cambridge, MA, 1990).
33. Supplementary data are available on Science Online at www.sciencemag.org/cgi/content/full/292/5515/290/DC1.
34. B. Tian, J. P. Rauschecker, *J. Neurophysiol.* **79**, 2629 (1998).
35. M. D. Hauser, *The Evolution of Communication* (MIT Press, Cambridge, MA, 1996).
36. R. Rajan, L. M. Aitkin, D. R. F. Irvine, J. McKay, *J. Neurophysiol.* **64**, 872 (1990).
37. J. P. Rauschecker, M. Korte, *J. Neurosci.* **13**, 4538 (1993).
38. The help of A. Lord, E. MacStravic, and C. Silver with recording and animal care is acknowledged gratefully. M. Hauser provided the monkey calls. Supported by U.S. Department of Defense (grant DAMD17-93-V-3018) and NIH (grants R01-DC03489 and R03-DC03845 to J.P.R. and B.T., respectively).

10 January 2001; accepted 8 March 2001

G Protein $\beta\gamma$ Subunit-Mediated Presynaptic Inhibition: Regulation of Exocytotic Fusion Downstream of Ca^{2+} Entry

Trillium Blackmer,^{1,3} Eric C. Larsen,⁵ Michiko Takahashi,² Thomas F. J. Martin,⁵ Simon Alford,^{2,4*} Heidi E. Hamm^{1,3,*†}

The nervous system can modulate neurotransmitter release by neurotransmitter activation of heterotrimeric GTP-binding protein (G protein)-coupled receptors. We found that microinjection of G protein $\beta\gamma$ subunits ($G\beta\gamma$) mimics serotonin’s inhibitory effect on neurotransmission. Release of free $G\beta\gamma$ was critical for this effect because a $G\beta\gamma$ scavenger blocked serotonin’s effect. $G\beta\gamma$ had no effect on fast, action potential-evoked intracellular Ca^{2+} release that triggered neurotransmission. Inhibition of neurotransmitter release by serotonin was still seen after blockade of all classical $G\beta\gamma$ effector pathways. Thus, $G\beta\gamma$ blocked neurotransmitter release downstream of Ca^{2+} entry and may directly target the exocytotic fusion machinery at the presynaptic terminal.

A number of neurotransmitters have been shown to modulate release from presynaptic terminals (1, 2) through activation of a G

protein-coupled receptor (GPCR) (3, 4). The two arms of activated G proteins, $G\alpha$ and $G\beta\gamma$, may exert their modulatory effect by

Downloaded from www.sciencemag.org on August 20, 2007